Supporting Information

Diversified antibiotic resistance and sensitivity patterns induced by quaternary ammonium compounds

Kun Yang [1,2,4], Huijie Lu [1,3], Lizhong Zhu (✉) [1,2,4]

1 State Key Laboratory of Soil Pollution Control and Safety, Zhejiang University, Hangzhou 310058, China

2 Department of Environmental Science, College of Environmental and Resource Sciences, Zhejiang University, Hangzhou 310058, China

3 Department of Environmental Engineering, College of Environmental and Resource Sciences, Zhejiang University, Hangzhou 310058, China

4 Zhejiang Provincial Key Laboratory of Organic Pollution Process and Control, Zhejiang University, Hangzhou 310058, China

✉ Corresponding author
E-mail: zlz@zju.edu.cn

Supplemental Methods

Collection of activated sludge: The activated sludge samples utilized in this study were obtained from the aeration tank of a municipal WWTP located in Hangzhou, China. By using 500 mL sterile polyethylene bottles (JET, Shanghai, China), mixed liquor samples were obtained at a depth of 20 cm below the water surface to avoid interference from surface scum or bottom sediments. Immediately following collection, samples were stored in portable coolers (4℃, Frestech, Xinxiang, China) to suppress microbial activity and prevent sample deterioration, then promptly transported to the laboratory for subsequent analysis. The MLSS was determined according to gravimetric methods (Yi et al., 2021). Briefly, 10 mL (V_0, mL) of homogenized sludge sample was filtered through pre-weighed quantitative filter paper (W_1, g) at constant speed. The filter paper with retained solids was then dried at 105℃ for 2 h to completely remove moisture. After drying, the filter paper was transferred to a desiccator and cooled for 30 min to reach room temperature before weighing (W_2, g). The MLSS concentration was calculated using the following equation: $\mathrm{MLSS(mg/L)}=\frac{W_2-W_1}{V}\times10^6$

Isolation methods of *E. coli*: The isolation of *E. coli* was performed using TBX agar (Haibo, Qingdao, China), a selective chromogenic medium containing 5-bromo-4-chloro-3-indolyl-*β*-D-glucuronide (X-Gluc) as the enzyme substrate. The medium specifically differentiates *E. coli* through *β*-glucuronidase activity, which hydrolyzes X-Gluc to produce blue-green colonies. The incorporated bile salts selectively inhibit Gram-positive bacteria, while other Gram-negative bacteria lacking this enzymatic activity form colorless or yellow colonies. The isolation methods consisted of the following steps: First, activated sludge suspensions were filtered through 0.45 μm membranes (Biosharp, Hefei, China) to remove particulate matter. Then, 50 μL of the filtrate was spread evenly onto TBX agar plates prepared according to the manufacturer's instructions. Serial dilutions were performed to ensure isolated colony formation. The inoculated plates were incubated at 37℃ for 24 h. After incubation, a single blue-green colony (presumptive *E. coli*) was randomly selected and inoculated into 5 mL of liquid LB medium for pre-culture (5 d, 37℃). The culture was then streaked onto LB agar plates for colony isolation. A single colony was randomly picked as the wild-type strain for subsequent experiments (Yu et al., 2024).

Intracellular ROS production: ROS production in bacteria was quantified by flow cytometry (B75442, Beckman Coulter, Suzhou, China) using the 2′,7′-dichlorodihydrofluorescein diacetate (DCFH-DA, Solarbio, Beijing, China) (Jin et al., 2018). Specifically, the bacterial suspension with OD600 of 0.5 was prepared in a 1.5 mL test tube and then incubated at 37℃ with 20 μmol/L DCFH-DA and different concentrations of TTAC for 20 min. After centrifuging twice at 6000 r/min at 25℃ for 1 min to wash away the remaining probes, the fluorescence intensity was detected by flow cytometry using fluorescence channel FITC with a gain value of 2500.

Mutation frequency: The mutation frequency was measured by plate counting method (Jin et al., 2018). After 20 d of exposure to different concentrations of TTAC, 60 μL of each cell culture was taken and incubated on LB agar containing 0.125 mg/L NOR (2×MIC) at 37℃ for 24 h to screen for antibiotic resistant bacteria, and then the number of colonies were counted. Colonies grown on antibiotic supplement plates were considered resistant to the NOR. The mutation frequency was

calculated by dividing the number of resistant colonies by the total number of bacteria, which was calculated by LB agar without antibiotic.

Membrane depolarization assay: The membrane depolarization test was carried out using 3,3-dipropylthiadicarbocyanine iodide ($DiSC_3(5)$, MedChemExpress, New Jersey, USA)) (Wang et al., 2022). The bacterial cells in logarithmic phase were collected and resuspended with PBS to obtain an OD600 of 0.5. The fluorescent probe $DiSC_3(5)$ was diluted to a concentration of 5×10^{-6} μmol/L and subsequently introduced into the reaction system. After incubated in the dark for 20 min, the fluorescence intensity was continuously monitored using a microplate reader (Spark, Tecan, Männedorf, Switzerland) with an excitation wavelength of 622 nm and an emission wavelength of 670 nm. At the 4th minute of measurement, different concentrations of TTAC were added to the reaction system and measured fluorescence intensity every 2 min for a total of 20 min. Each treatment group had three biological replicates and two technical replicates. The depolarization process of cells was reflected by observing the change of fluorescence intensity under TTAC exposure.

Proton motive force assay: The pH-sensitive fluorescence probe BCECF-AM (MedChemExpress, New Jersey, USA) was used to monitor the change of PMF (Wang et al., 2022). The bacterial cells in logarithmic phase were collected and resuspended with PBS to obtain an OD600 of 0.5. The fluorescence probe BCECF-AM mother solution was diluted with HEPES, and then probes with a final working concentration of 2.5×10^{-6} μmol/L and different concentrations of TTAC were added to the reaction system. After incubating together in darkness for 30 min, the fluorescence intensity was monitored using a microplate reader (Spark, Tecan, Männedorf, Switzerland) with an excitation wavelength of 488 nm and an emission wavelength of 535 nm. Experimental data were analyzed from three biological replicates and two technique replicates.

Intracellular ATP levels: Intracellular ATP levels of *E. coli* were determined using an ATP Assay Kit (Beyotime, Shanghai, China) (Liu et al., 2020). The bacterial cells in logarithmic phase were collected and resuspended with PBS to obtain an OD600 of 0.5. After treating by various concentrations of TTAC for 1 h, bacterial cultures were centrifuged at 12000 g at 4℃ for 5 min, and the supernatant was removed. Added 200 μL of lysate, swirled to ensure sufficient cleavage of bacterial precipitate, centrifuged, and prepared supernatant for subsequent determination. The diluted ATP detecting solution was added to the black 96-well plate and left it at room temperature for 5 min to consume all the background ATP. Subsequently, the supernatants were added to the well, mixed quickly, and the luminescence was measured by multifunctional microplate reader (Spark, Tecan, Männedorf, Switzerland). All experiments were performed on an ice bath, and with two biological replicates and two technical replicates. Total ATP levels in samples were calculated based on the standard curve of luminescence signals versus concentrations of ATP standard solution.

Efflux pump activity: Ethidium bromide (EtBr, MedChemExpress, New Jersey, USA) efflux assay was performed based on previous study (Wang et al., 2022). *E. coli* with OD600 of 0.5 was co-incubated with 5 mmol/L EtBr and different concentrations of TTAC at 37℃, 200 r/min for 1h, and then centrifuged at 4℃ and 5000 r/min for 1 min. After EtBr adsorbed on cell surface was washed off, the microspheres were collected and re-suspended in fresh LB. Under excitation wavelength of 530 nm and emission wavelength of 600 nm, the residual EtBr concentration was

monitored after 60 min. Each treatment group had three biological replicates and two technical replicates.

Outer membrane permeability: The permeability of the bacterial outer membrane was measured using the fat-soluble fluorescent dye 1-N-phenylnaphthylamine (NPN, MedChemExpress, New Jersey, USA) (Liu et al., 2020). The bacterial cells in logarithmic phase were collected and resuspended with PBS to obtain an OD600 of 0.5. NPN dye and different concentrations of TTAC were added to brown test tubes and incubated in darkness for 25 min. The fluorescence intensity was detected by flow cytometry (B75442, Beckman Coulter, Suzhou, China) using fluorescence channel V450 with a gain value of 1000.

Intracellular CEF levels: The intracellular CEF accumulation was measured by high performance liquid chromatography (HPLC, Agilent, California, USA). The detailed chromatographic conditions were as follows (Valassis et al., 1999): C18 column (250mm × 4.6mm, 5μm), mobile phase consisted of A: pure acetonitrile, B: 0.015 mol/L sodium pentane sulfonic acid (pH = 4, adjusted by phosphoric acid), detection wavelength was 258 nm, flow rate was 1 mL/min, sample size was 20 μL, column temperature was 25℃. After 20 d of exposure to different concentrations of TTAC, 1 mL of bacterial suspension was collected in test tubes, centrifuged to remove the medium, then re-suspended with normal saline containing 0.12 mg/L CEF (C_{tot}) and diluted to OD600 of 0.5. The tubes were incubated at 37℃ for 60 min. After centrifuging at 12000 r/min at 4℃ for 5 min, the supernatant was used to detected the reduced antibiotic concentration in the solution (C_{sol}). Then washed with normal saline for 2 times, the washing solution was combined and concentrated 4 times to detected the cell surface adhesion concentration (C_{adh}). The tube without bacteria was used as a control group to determine the natural degradation concentration of antibiotic (C_{deg}). The intracellular CEF concentration (C_{int}) was calculated indirectly by the following formula:

$$C_{int}=C_{tot}-C_{deg}-C_{sol}-C_{adh}/4$$

DNA extraction and Whole-Genome resequencing: Evolved *E. coli* populations were collected after 20 d of QACs exposure, as well as on days 5, 10, 15, and 20 from the TTAC-treated group. By using the E.Z.N.A. Tissue DNA kit (Omega Bio-Tek, Norcross, GA, USA), total DNA were extracted and used for sequencing (Yu et al., 2024). For Illumina pair-end sequencing, at least 3μg genomic DNA was used for sequencing library construction for each sample. Paired-end libraries with insert sizes of ~450bp were prepared following Illumina's standard genomic DNA library preparation procedure. Purified genomic DNA is sheared into smaller fragments with a desired size by Covaris, and T4 DNA polymerase was applied to generate blunt ends. After adding an 'A' base to the 3′ end of the blunt phosphorylated DNA fragments, adapters are ligated to the ends of the DNA fragments. The desired fragments can be purified through gel-electrophoresis, then selectively enriched and amplified by PCR. The index tag could be introduced into the adapter at the PCR stage as appropriate followed by a library quality test. At last, the quantified Illumina pair-end libraries sequenced by Illumina NovaSeq 6000 platform (150bp × 2, Biozeron Biotechnology Co., Ltd, Shanghai, China). The raw paired end reads were trimmed and quality controlled by Trimmomatic with parameters (SLIDINGWINDOW:4:15 MINLEN:75) (version 0.36). The clean sequencing reads are aligned to the reference genome sequence using BWA software (bwa mem -k 32). Sequence Alignment Map (SAM) format files were imported into SAMtools for sorting and merging and into Picard (version 1.92) to remove duplicated reads. The

sequencing depth and coverage were calculated based on the alignments by custom perl scripts. The valid BAM file was used to detect SNPs and short InDel by GATK (version 4.1.2.0) "HaplotypeCaller" function. Followed variant call format (VCF) files were generated by quality filtering (VCFtools, VariantFiltration with parameters: QD < 2.0 || FS > 60.0 || MQ < 40.0 || SOR > 10.0). When the gene annotation file of reference genome is provided, the annotation of detected variations can be performed by ANNOVAR, including SNP and InDel.

RNA extraction and transcriptomic analysis: Total RNA was extracted from the population suspensions collected 20 d after exposure to 1 mg/L TTAC by using TRIzol® Reagent (Thermo Fisher Scientific, Hangzhou, China) (Liu et al., 2021). Then RNA quality was determined using 2100 Bioanalyser (Agilent, California, USA) and quantified using the ND-2000 (NanoDrop, Wilmington, USA). High-quality RNA sample (OD260/280 = 1.8~2.2, OD260/230 ≥ 2.0, RIN ≥ 6.5, 28S:18S ≥ 1.0, > 10μg) is used to construct sequencing library. RNA-seq strand-specific libraries were prepared following TruSeq RNA sample preparation Kit from Illumina (San Diego, CA, USA), using 5μg of total RNA. After quantified by TBS380, Paired-end libraries were sequenced by Illumina NovaSeq 6000 sequencing (150bp × 2, Biozeron Biotechnology Co., Ltd, Shanghai, China). The raw paired end reads were trimmed and quality controlled by Trimmomatic with parameters (SLIDINGWINDOW:4:15 MINLEN:75). Then clean reads were separately aligned to reference genome with orientation mode using Rockhopper software. To identify DEGs between the two different samples, the expression level for each transcript was calculated using the fragments per kilobase of read per million mapped reads (RPKM) method. The edgeR was used for differential expression analysis. The DEGs between two samples were selected using the following criteria: the logarithmic of fold change was greater than 2 and the false discovery rate (FDR) should be less than 0.05. To understand the functions of the differential expressed genes, GO functional enrichment was carried out by Goatools. DEGs were significantly enriched in GO terms and metabolic pathways when their Bonferroni-corrected P-value was less than 0.05.

Supplemental Figures

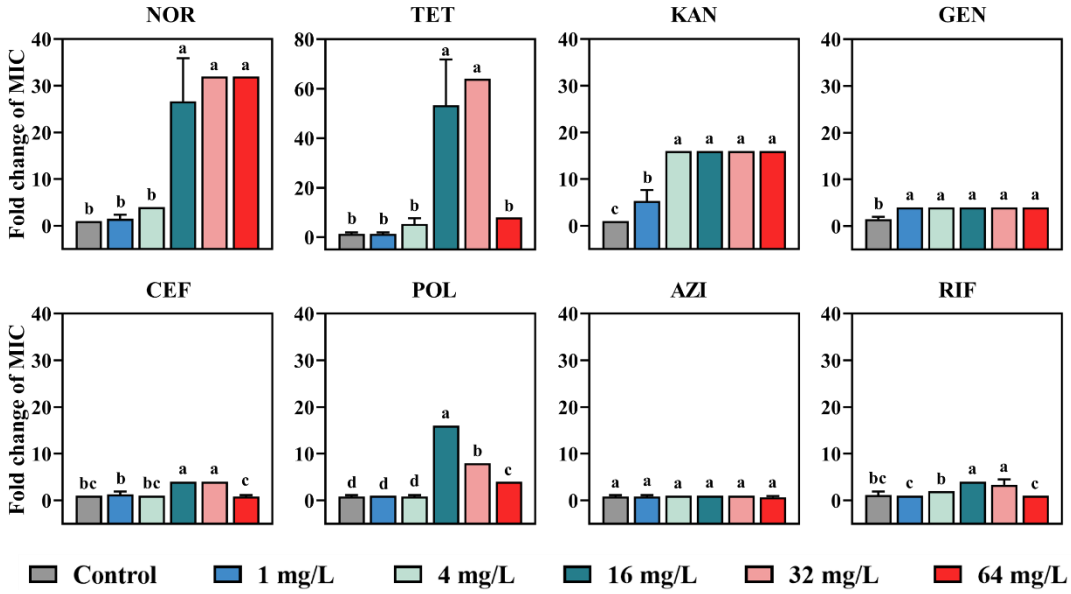

Fig. S1 The fold change of MIC against eight classes of antibiotics after 15 d of DDAC exposure in AS. The samples were obtained from three biological replicates. Different letters (a, b, c, d) indicated significant differences between groups ($p < 0.05$).

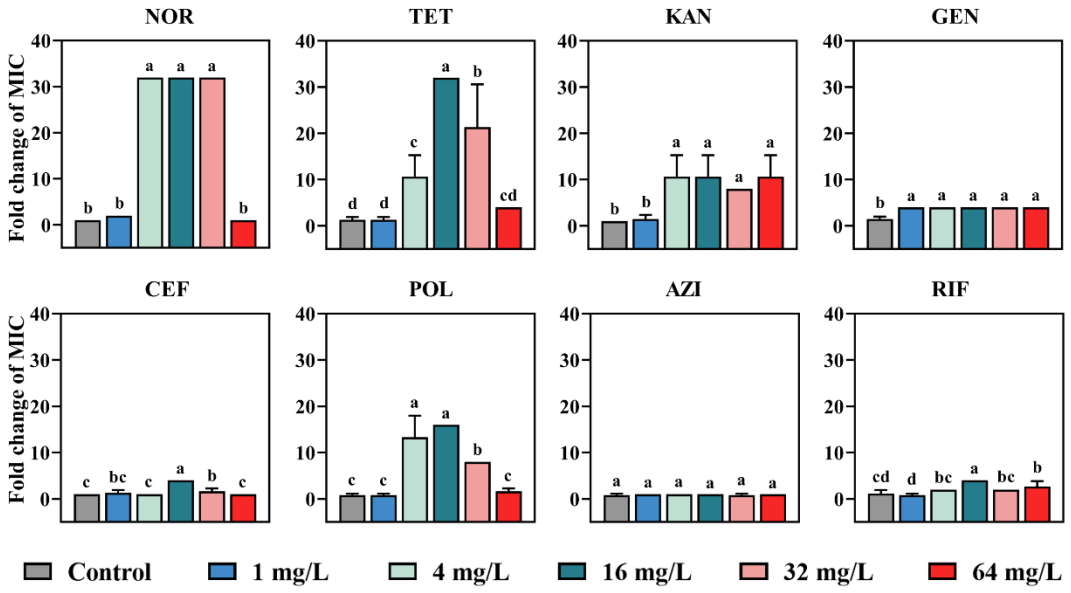

Fig. S2 The fold change of MIC against eight classes of antibiotics after 15 d of DDBAC exposure in AS. The samples were obtained from three biological replicates. Different letters (a, b, c, d) indicated significant differences between groups ($p < 0.05$).

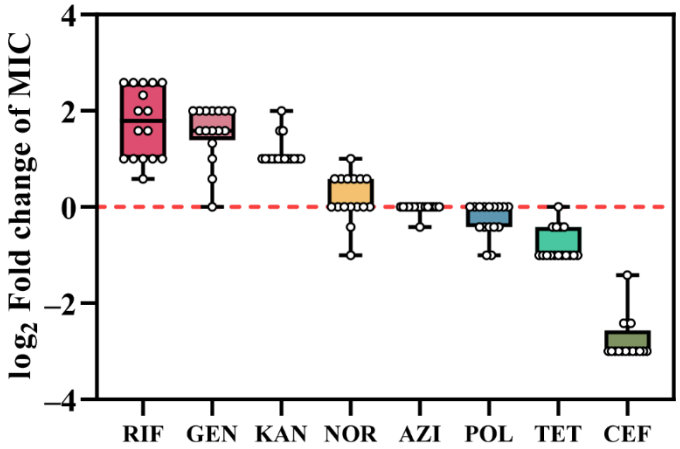

Fig. S3 Distribution of MICs for each treatment group against the eight antibiotics at the 20th d of 16 types of QACs exposure.

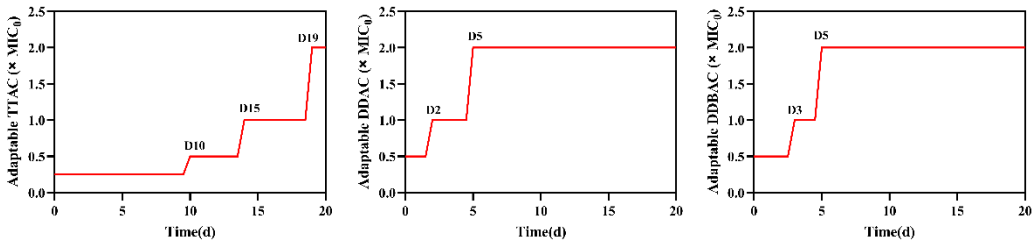

Fig. S4 The highest concentrations of three representative QACs (TTAC, DDAC, DDBAC) to which *E. coli* could adapt during successive passaging, expressed as fold changes relative to their initial MICs (MIC_0: 64, 8, and 32 mg/L, respectively).

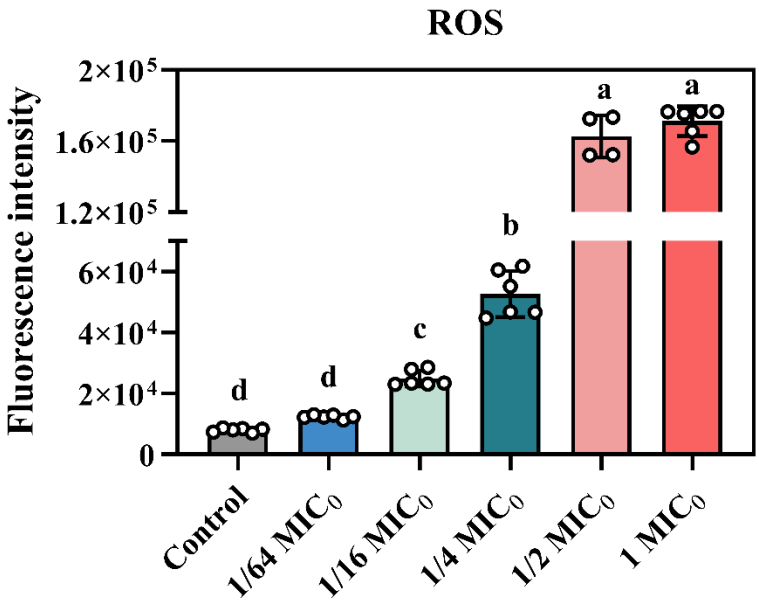

Fig. S5 Intracellular ROS production measured by fluorescent probe DCFH-DA after 8 h exposure to different concentrations of TTAC. The samples were obtained from three biological replicates and two technical replicates**.** Different letters (a, b, c, d) indicated significant differences between groups ($p < 0.05$).

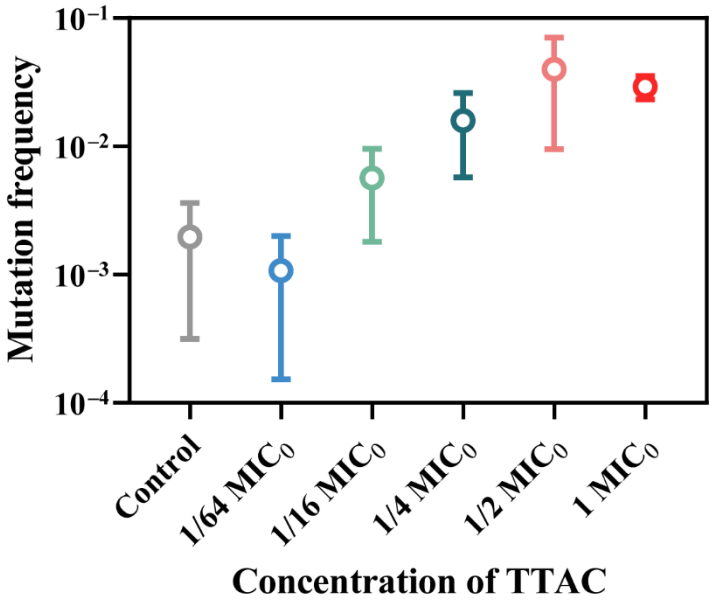

Fig. S6 The Mutation frequency of *E. coli* at the end exposure experiment to different concentrations of TTAC.

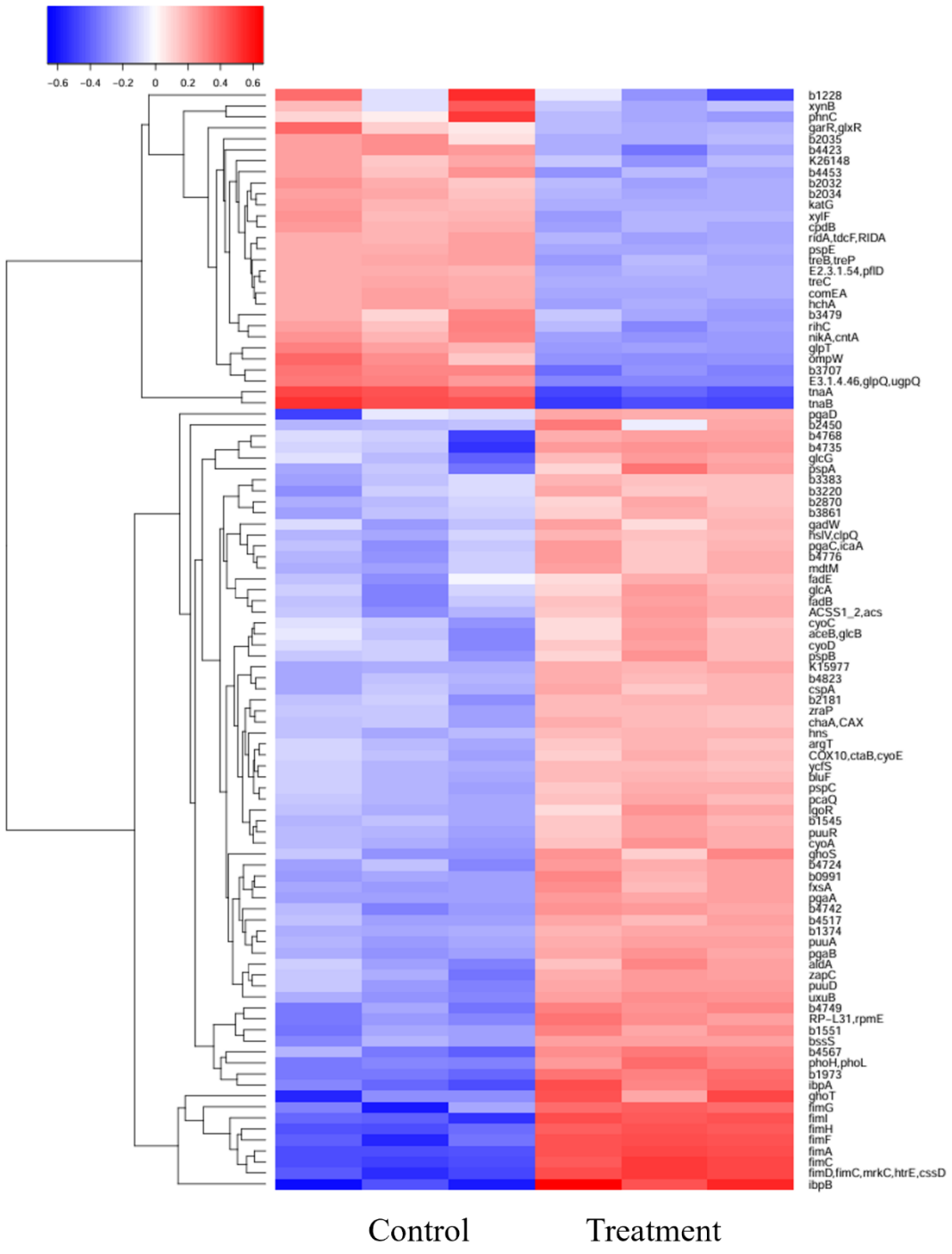

Fig. S7 Clustering analysis of specific DEGs with FDR < 0.05 and $|\log_2$ Fold Change$| \geq 1$. Lanes 1-3 represented the three biological replicates of the wild-type and lanes 4-6 represented *E. coli* after 1 mg/L TTAC treatment.

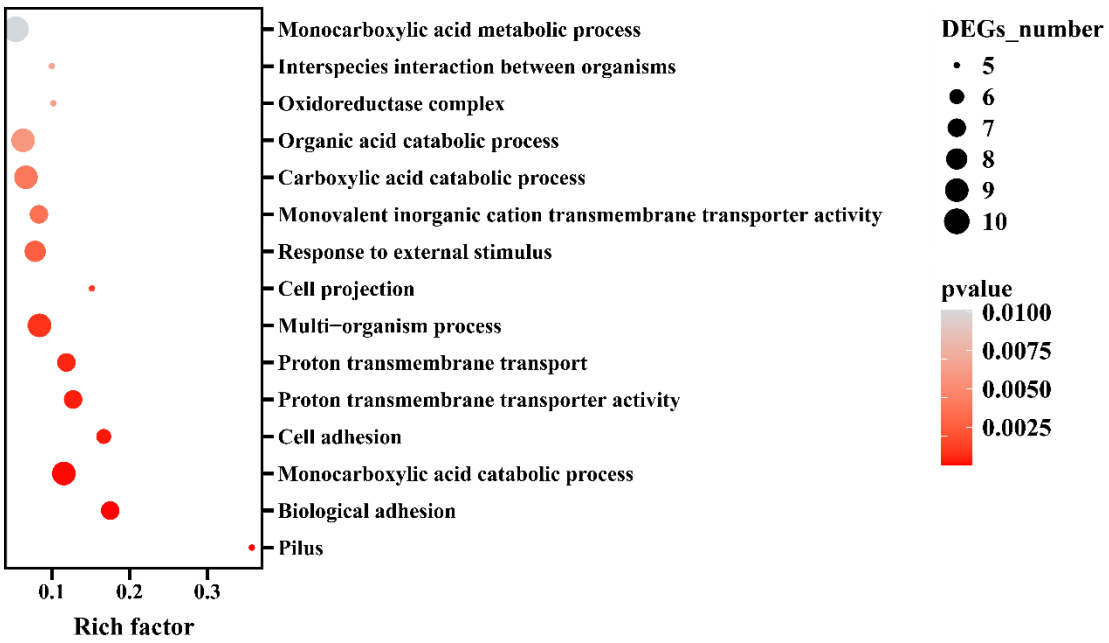

Fig. S8 Upregulated DEGs (FDR < 0.05 and $\log_2$ Fold change > 1), the 15 most significant enriched pathways were shown.

Supplemental Tables

Table S1 Types and concentrations of QACs in WWTPs (water μg/L, sludge μg/kg).

Sample	Country	Range of concentration	Reference
wastewater	Germany	DADMACs: 0~830	(Gerike et al., 1994)
wastewater	China	ATMACs: 67~102	(Shrivas and Wu, 2007)
wastewater	Austria	BACs: 50~6030	(Kümmerer et al., 1997)
Influent	America	QACs: 12.8~173.8	(Mahony et al., 2023)
Influent	Austria	ATMACs: 9.75~34.3; DADMACs: 15.5~292.3; BACs: 35.2~306.8	(Clara et al., 2007)
Influent	Austria	ATMACs: 2.4~7.1; DADMACs: 2.27~4010; BACs: 1.23~6105	(Martínez et al., 2007)
Influent	Sweden	BACs: 2.2~40.1	(Östman et al., 2017)
Influent	China	BACs: 1.78~2.47	(Li et al., 2020)
Effluent	America	QACs: 0.4~6.6	(Pati and Arnold, 2020)
Effluent	Sweden	BACs: 0~0.4	(Östman et al., 2017)
Effluent	Europe	ATMACs: 0~14.6; DADMACs: 0~16.2; BACs: 0~78.1	(Kaj et al., 2014)
Effluent	America	QACs: 0~1.8	(Mahony et al., 2023)
River	China	ATMAC: 0~1.24	(Ding and Tsai, 2003)
River	Japan	DADMACs: 0.05~0.67	(Miura et al., 2008)
Sludge	Sweden	BACs: 13014~154110	(Östman et al., 2017)
Sludge	China	ATMACs: 400~294000; DADMACs: 640~343000; BACs: 900~191000	(Ruan et al., 2014)
Sludge	Europe	ATMACs: 14900~109400; DADMACs: 9300~56200; BACs: 0~2090	(Kaj et al., 2014)

Note. ATMACs: Alkyl trimethylammonium compounds; DADMACs: Dialkyl dimethyl ammonium compounds; BACs: Benzyl dimethylammonium compounds

Table S2 The specific composition of the synthetic wastewater (Smolders et al., 1994).

Nutrient element	Composition	Concentration (mg/L)
C	CH_3COONa	384.4
P	KH_2PO_4	49.4
N	$(NH_4)_2SO_4$	140
Ca	$CaCl_2·2H_2O$	14
Mg	$MgSO_4·7H_2O$	90
Fe	$FeCl_3·6H_2O$	0.45
B	H_3BO_3	0.045
Cu	$CuSO_4·5H_2O$	0.009
I	KI	0.054
Mn	$MnCl_2·4H_2O$	0.036
Mo	$Na_2MoO_4·2H_2O$	0.018
Zn	$ZnSO_4·7H_2O$	0.036
Co	$CoCl_2·6H_2O$	0.045
Buffer	EDTA	3

Table S3 The initial MICs of AS against three representative QACs and eight antibiotics (mg/L).

QACs	MIC_0	Antibiotic	MIC_0	Antibiotic	MIC_0
TTAC	64	NOR	16	CEF	32
DDAC	16	TET	8	POL	128
DDBAC	32	KAN	64	AZI	512
		GEN	128	RIF	64

Table S4 Abbreviations and structures of the 16 kinds of QACs used in this study.

Species	Abbreviation	Structure
Octanyl trimethyl ammonium chloride	ATMAC8	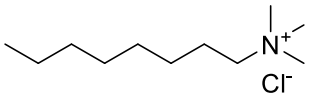
Decyl trimethyl ammonium chloride	ATMAC10	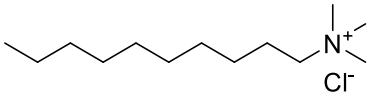
Dodecyl trimethyl ammonium chloride	ATMAC12	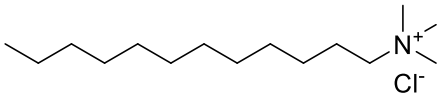
Tetradecyl trimethyl ammonium chloride	ATMAC14	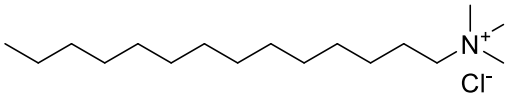
Cetyl trimethyl ammonium chloride	ATMAC16	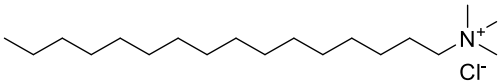
Octadecyl trimethyl ammonium chloride	ATMAC18	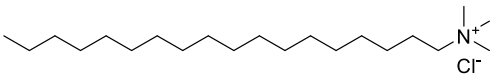
Didecyl dimethyl ammonium chloride	DADMAC10	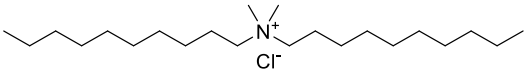
Didodecyl dimethyl ammonium chloride	DADMAC12	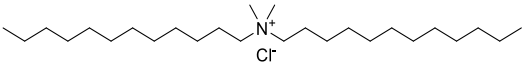
Didecyl dimethyl ammonium bromide	DADMAB10	
Dihexadecyl dimethyl ammonium bromide	DADMAC16	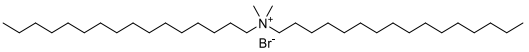
Dodecyl dimethyl benzyl ammonium chloride	DDBAC	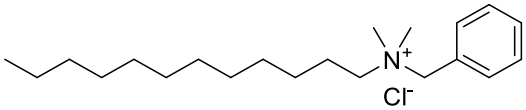
Dodecyl dimethyl benzyl ammonium bromide	DDBAB	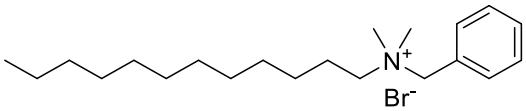
Cetyl trimethyl ammonium bromide	DADMAB16	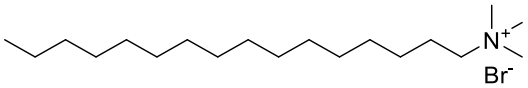
Cetylpyridine chloride	CPC	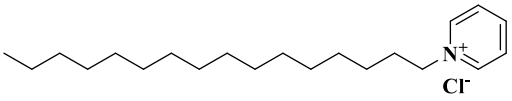
Domiphen bromide	DMPB	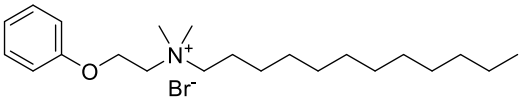

Species	Abbreviation	Structure
Benzethonium chloride	BC	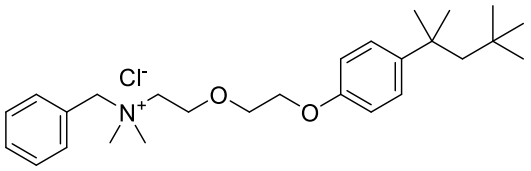

Table S5 The initial MICs of *E. coli* against 16 types of QACs and eight antibiotics (mg/L).

QACs	MIC_0	QACs	MIC_0	Antibiotic	MIC_0
ATMAC8	128	DADMAB10	4	NOR	0.0625
ATMAC10	128	DADMAC16	128	TET	2
ATMAC12	64	DDBAC	32	KAN	8
ATMAC14	64	DDBAB	16	GEN	2
ATMAC16	32	DADMAB16	64	CEF	0.5
ATMAC18	64	CPC	64	POL	4
DADMAC10	8	DMPB	32	AZI	256
DADMAC12	64	BC	32	RIF	2

Table S6 The meanings of CDK molecular descriptors and the Pearson correlation coefficient between the MICs of NOR and CEF.

Descriptor	Meaning	NOR	CEF
khs.aasN	Number of nitrogen-containing fragments	−0.20407	0.305167
C1SP2	Primary carbon atoms with SP^2 hybridization	−0.20407	0.305167
VCH.7	Charge distribution or electrostatic potential parameters	−0.2901	0.302334
ECCEN	Molecular eccentricity	0.040967	0.275279
VCH.6	Charge distribution or electrostatic potential parameters	−0.31495	0.257079
SCH.6	Number of sulfur-containing groups	−0.29903	0.219849
khs.aaCH	Number of consecutive methylene (-CH-) fragments	−0.29898	0.219751
nAtomP	Total number of polar atoms	−0.29478	0.181961
HybRatio	Average hybridization state ratio of atoms	0.285264	−0.20501
ALogp2	Hydrophobicity parameters	0.378519	−0.2459
VP.5	Volatility-related parameters	0.32726	−0.25887
fragC	Number of discontinuous fragments	0.307886	−0.27975
MDEC.12	Molecular distance edge connectivity index	0.309177	−0.28453
nAtomLC	Number of long-chain atoms	0.25959	−0.29771
VP.6	Volatility-related parameters	0.363762	−0.30152
nBase	Number of basic groups	0.204072	−0.30517
khs.ssssN	Number of fully saturated nitrogen atoms	0.204072	−0.30517

Descriptor	Meaning	NOR	CEF
VP.7	Volatility-related parameters	0.380555	−0.31242
Kier2	Three-dimensional topological shape index	0.317093	−0.31775
XLogP	Octanol-water partition coefficient based on atomic contribution method	0.332914	−0.31921
C2SP3	Secondary carbon atoms with SP^3 hybridization	0.362019	−0.32782
MW	Molecular weight	0.238203	−0.33174
ALogP	Octanol-water partition coefficient (logP)	0.377665	−0.34529
khs.ssCH2	Number of consecutive methylene (-CH_2-) fragments	0.370191	−0.34614
nRotB	Number of rotatable bonds	0.33186	−0.34881
Kier3	Three-dimensional topological shape index	0.300672	−0.36461
ATSm1	Molecular surface area or topological polarity	0.340058	−0.48214

Table S7 Mutations in strains from different treatment groups.

Sample	All-SNP	Hom	Het	All-indel	Deletion	Insertion
Wild-type	0	0	0	4	2	2
D5	0	0	0	4	2	2
D10	0	0	0	4	2	2
D15	0	0	0	4	2	2
D20	0	0	0	4	2	2
ATMAC8	0	0	0	4	2	2
ATMAC10	0	0	0	4	2	2
ATMAC12	0	0	0	4	2	2
ATMAC16	0	0	0	4	2	2
DADMAC10	0	0	0	4	2	2
DADMAC12	0	0	0	4	2	2
DADMAB10	0	0	0	4	2	2
DADMAC16	0	0	0	4	2	2
DDBAC	0	0	0	4	2	2
DDBAB	0	0	0	4	2	2
DMPB	0	0	0	4	2	2

Table S8 The specific mutation information.

Mutation	Region	Gene	Function
-T	CDS	cspC	transcription antiterminator
+ TA	CDS	rpoS	RNA polymerase sigma factor RpoS
-GG	CDS	glpD	glycerol-3-phosphate dehydrogenase
+ CG	downstream	cds-NP_418501.1-cds-NP_418502.1	/

Table S9 DEGs related to drug catabolic process after 1 mg/L TTAC exposure.

ID	**Gene**	**Function**	**Log_2 FC**	**FDR**
b0331	prpB	Methylisocitrate lyase	−1.16778	0.001114
b0334	prpD	2-methylcitrate dehydratase	−1.2751	0.000109
b0512	allB	allantoinase AllB	−1.16132	0.000454
b0514	glxK	glycerate kinase 1	−1.08432	0.001619
b0903	pflD	formate acetyltransferase 1	−1.3369139	3.10E-06
b1007	rutF	pyrimidine utilization flavin reductase F	−1.20438	0.000574
b1009	rutD	Putative aminoacrylate hydrolase RutD	−1.05688	0.003884
b1010	rutC	pyrimidine utilization protein C	−1.28677	0.002358
b1011	rutB	putative synthetase	−1.10217	0.002832
b1012	rutA	pyrimidine utilization protein A	−1.14774	0.001259
b3125	garR	tartronate semialdehyde reductase	−1.41936	2.70E-06
b3126	garL	5-keto-4-deoxy-D-glucarate aldolase	−1.14724	0.000575
b3222	nanK	N-acetylmannosamine kinase	−1.152048	0.000877936
b3942	katG	catalase-peroxidase HPI	−1.400699	8.26E-07

Table S10 DEGs related to NADH dehydrogenase complex after 1 mg/L TTAC exposure.

ID	Gene	Function	Log_2 FC	FDR
b2276	nuoN	NADH-quinone oxidoreductase subunit N	−1.15644	0.000151
b2277	nuoM	NADH-quinone oxidoreductase subunit M	−1.13183	0.000209
b2278	nuoL	NADH-quinone oxidoreductase subunit L	−1.06992	0.000514
b2280	nuoJ	NADH: ubiquinone oxidoreductase subunit J	−1.11425	0.000333
b2281	nuoI	NADH: ubiquinone oxidoreductase, chain I protein	−1.07376	0.000561
b2282	nuoH	NADH-quinone oxidoreductase subunit NuoH	−1.12192	0.000243
b2283	nuoG	NADH dehydrogenase I chain G	−1.10271	0.000299

Table S11 DEGs related to antibiotic resistance after 1 mg/L TTAC exposure.

Number	Gene	Log_2 Fold Change	Function
1	soxS	0.631261033	transcriptional repressor
2	soxR	1.129022402	transcriptional repressor
3	acrR	0.639269222	transcriptional repressor
4	marR	0.407970128	transcriptional repressor
5	mdtM	1.29916595	efflux pump
6	mdtL	−0.707241804	efflux pump
7	mdtB	−0.780223156	efflux pump
8	mdtC	−1.095338379	efflux pump
9	mdtD	−0.999781443	efflux pump
10	cusB	−0.661598809	efflux pump
11	cusA	−0.799995058	efflux pump
12	emrB	−0.85934266	efflux pump
13	uhpT	−1.016487285	major facilitator superfamily

Number	Gene	Log_2 Fold Change	Function
14	uhpC	−0.645338379	major facilitator superfamily
15	uhpB	−0.788527592	major facilitator superfamily
16	mhpT	−0.791382874	major facilitator superfamily
17	ssuB	−0.95077852	ABC transporter
18	ssuC	−0.906895006	ABC transporter
19	ssuD	−1.099824901	ABC transporter
20	ssuE	−0.98283911	ABC transporter
21	phnP	−1.084693939	ABC transporter
22	phnO	−0.993233153	ABC transporter
23	phnN	−0.925828129	ABC transporter
24	phnM	−1.097156694	ABC transporter
25	phnL	−1.142279591	ABC transporter
26	phnK	−0.947378338	ABC transporter
27	phnJ	−1.037922533	ABC transporter
28	phnI	−1.001842259	ABC transporter
29	phnH	−1.09096274	ABC transporter
30	phnH	−1.47359131	ABC transporter
31	phnF	−1.426086622	ABC transporter
32	phnD	−1.082844914	ABC transporter
33	phnC	−1.792731616	ABC transporter
34	phnA	0.44560372	ABC transporter
35	tauA	−1.062087176	ABC transporter
36	tauB	−1.162350941	ABC transporter

Number	Gene	Log_2 Fold Change	Function
37	tauC	−1.110236266	ABC transporter
38	nikA	−1.749434224	ABC transporter
39	nikB	−1.242354721	ABC transporter
40	nikC	−1.279207566	ABC transporter
41	nikD	−1.431463688	ABC transporter
42	nikE	−1.138051973	ABC transporter
43	nikR	−0.799789353	ABC transporter
44	livM	−0.888832218	ABC transporter
45	yphD	−0.777954549	ABC transporter
46	yphE	−1.102794642	ABC transporter
47	yphF	−1.311949952	ABC transporter
48	modA	−0.642750947	ABC transporter
49	modB	−0.749735662	ABC transporter
50	modC	−0.622384655	ABC transporter
51	hycG	−0.950359936	formate hydrogenlyase
52	hycF	−1.152387099	formate hydrogenlyase
53	hycE	−0.803703822	formate hydrogenlyase
54	hycD	−1.036762175	formate hydrogenlyase
55	hycC	−1.114786538	formate hydrogenlyase
56	recA	0.458551461	DNA replication and repair
57	recN	0.813051717	DNA replication and repair
58	recE	−0.924232492	DNA replication and repair
59	recD	−0.720019166	DNA replication and repair

Number	Gene	Log_2 Fold Change	Function
60	ruvC	−0.647984607	DNA replication and repair
61	uvrA	0.791802295	DNA replication and repair
62	frdD	0.530010131	DNA replication and repair
65	sulA	0.55112976	DNA replication and repair
66	umuD	0.371368663	DNA replication and repair
67	dinI	0.658546875	DNA replication and repair

References

Clara M, Scharf S, Scheffknecht C, Gans O (2007). Occurrence of selected surfactants in untreated and treated sewage. Water Research, 41(19): 4339–4348 doi:10.1016/j.watres.2007.06.027

Ding W H, Tsai P C (2003). Determination of alkyltrimethylammonium chlorides in river water by gas chromatography/ion trap mass spectrometry with electron impact and chemical ionization. Analytical Chemistry, 75(8): 1792–1797 doi:10.1021/ac020536y

Gerike P, Klotz H, Kooijman J G A, Matthijs E, Waters J (1994). The determination of dihardenedtallowdimethyl ammonium compounds (DHTDMAC) in environmental matrices using trace enrichment techniques and high performance liquid chromatography with conductometric detection. Water Research, 28(1): 147–154 doi:10.1016/0043-1354(94)90128-7

Jin M, Lu J, Chen Z Y, Nguyen S H, Mao L K, Li J, Yuan Z G, Guo J H (2018). Antidepressant fluoxetine induces multiple antibiotics resistance in Escherichia coli via ROS-mediated mutagenesis. Environment International, 120: 421–430 doi:10.1016/j.envint.2018.07.046

Kaj L, Wallberg P, Brorström-Lundén E (2014). Quaternary ammonium compounds: Analyses in a Nordic cooperation on screening. Berlin: ResearchGate

Kümmerer K, Eitel A, Braun U, Hubner P, Daschner F, Mascart G, Milandri M, Reinthaler F, Verhoef J (1997). Analysis of benzalkonium chloride in the effluent from European hospitals by solid-phase extraction and high-performance liquid chromatography with post-column ion-pairing and fluorescence detection. Journal of Chromatography. A, 774(1–2): 281–286 doi:10.1016/S0021-9673(97)00242-2

Li W L, Zhang Z F, Sparham C, Li Y F (2020). Validation of sampling techniques and SPE-UPLC/MS/MS for home and personal care chemicals in the Songhua Catchment, Northeast China. Science of the Total Environment, 707: 136038 doi:10.1016/j.scitotenv.2019.136038

Liu Y, Jia Y, Yang K, Li R, Xiao X, Zhu K, Wang Z (2020). Metformin restores tetracyclines susceptibility against multidrug resistant bacteria. Advanced Science (Weinheim, Baden-Wurttemberg, Germany), 7(12): 1902227 doi:10.1002/advs.201902227

Liu Y, Tong Z, Shi J, Jia Y, Deng T, Wang Z (2021). Reversion of antibiotic resistance in multidrug-resistant pathogens using non-antibiotic pharmaceutical benzydamine. Communications Biology, 4(1): 1328 doi:10.1038/s42003-021-02854-z

Mahony A K, Mcnamara P J, Arnold W A (2023). Quaternary ammonium compounds (QACs) in wastewater influent and effluent throughout the COVID-19 pandemic. Environmental Science & Technology, 57(48): 20148–20158 doi:10.1021/acs.est.3c04413

Martínez-Carballo E, Sitka A, González-Barreiro C, Kreuzinger N, Fürhacker M, Scharf S, Gans O (2007). Determination of selected quaternary ammonium compounds by liquid chromatography with mass spectrometry. Part I. Application to surface, waste and indirect discharge water samples in Austria. Environmental Pollution, 145(2): 489–496 doi:10.1016/j.envpol.2006.04.033

Miura K, Nishiyama N, Yamamoto A (2008). Aquatic environmental monitoring of detergent surfactants. Journal of Oleo Science, 57(3): 161–170 doi:10.5650/jos.57.161

Östman M, Lindberg R H, Fick J, Björn E, Tysklind M (2017). Screening of biocides, metals and antibiotics in Swedish sewage sludge and wastewater. Water Research, 115: 318–328 doi:10.1016/j.watres.2017.03.011

Pati S G, Arnold W A (2020). Comprehensive screening of quaternary ammonium surfactants and ionic liquids in wastewater effluents and lake sediments. Environmental Science. Processes & Impacts, 22(2): 430–441 doi:10.1039/C9EM00554D

Ruan T, Song S, Wang T, Liu R, Lin Y, Jiang G (2014). Identification and composition of emerging quaternary ammonium compounds in municipal sewage sludge in China. Environmental Science & Technology, 48(8): 4289–4297 doi:10.1021/es4050314

Shrivas K, Wu H F (2007). A rapid, sensitive and effective quantitative method for simultaneous determination of cationic surfactant mixtures from river and municipal wastewater by direct combination of single-drop microextraction with AP-MALDI mass spectrometry. Journal of Mass Spectrometry, 42(12): 1637–1644 doi:10.1002/jms.1266

Smolders G J F, Van Der Meij J, Van Loosdrecht M C M, Heijnen J J (1994). Stoichiometric model of the aerobic metabolism of the biological phosphorus removal process. Biotechnology and Bioengineering, 44(7): 837–848 doi:10.1002/bit.260440709

Valassis I N, Parissi-Poulou M, Macheras P (1999). Quantitative determination of cefepime in plasma and vitreous fluid by high-performance liquid chromatography. Journal of Chromatography. Biomedical Applications, 721(2): 249–255 doi:10.1016/S0378-4347(98)00468-X

Wang C, Lu H, Li X, Zhu Y, Ji Y, Lu W, Wang G, Dong W, Liu M, Wang X, Chen H, Tan C (2022). Identification of an anti-virulence drug that reverses antibiotic resistance in multidrug resistant bacteria. Biomedicine and Pharmacotherapy, 153: 113334 doi:10.1016/j.biopha.2022.113334

Yi X, Zhong H, Xie M, Wang X (2021). A novel forward osmosis reactor assisted with microfiltration for deep thickening waste activated sludge: performance and implication. Water Research, 195: 116998 doi:10.1016/j.watres.2021.116998

Yu J X, Lu H J, Zhu L Z (2024). Mutation-driven resistance development in wastewater E. coli upon low-level cephalosporins: Pharmacophore contribution and novel mechanism. Water Research, 252: 121235 doi:10.1016/j.watres.2024.121235